SINR and Rate Meta Distributions for HCNs with Joint Spectrum Allocation and Offloading

Na Deng, *Member, IEEE*, and Martin Haenggi, *Fellow, IEEE*

Abstract

This paper focuses on the meta distributions of the signal-to-interference-plus-noise ratio (SINR) and user-perceived rate in heterogeneous cellular networks (HCNs) with multiple tiers of base stations. On the one hand, it is desirable to offload users to small cells to alleviate the congestion in macrocells; on the other hand, such offloading would in turn cause an SINR degradation of the offloaded users, which needs to be mitigated through interference avoidance based on resource partitioning. Thus, in consideration of both aspects, we provide a general framework for modeling and analyzing joint spectrum allocation and offloading in a HCN using the K-tier homogeneous independent Poisson model. With it, we derive the per-tier and overall moments of the conditional SINR and rate distribution given the point process, based on which the exact meta distributions are given. We show that the conventional SINR or rate performance evaluated at the typical user (averaging over all tiers and links in the HCN), by itself, is insufficient, and a much sharper version provided by the meta distribution is required in conjunction with the expected value to give a thorough assessment of the benefits of joint resource partitioning and offloading in HCNs.

Index Terms

Stochastic geometry, heterogeneous cellular network, SINR, user-perceived rate, offloading, spectrum allocation.

Na Deng is with the School of Information and Communication Engineering, Dalian University of Technology (DLUT), Dalian, 116024, China (e-mail: dengna@dlut.edu.cn). Martin Haenggi is with the Dept. of Electrical Engineering, University of Notre Dame, Notre Dame 46556, USA (e-mail: mhaenggi@nd.edu).

Part of this work has been presented at the IEEE International Symposium on Personal, Indoor and Mobile Radio Communications in 2018 [1].

This work was supported by the National Natural Science Foundation of China under Grant 61701071, by the China Postdoctoral Science Foundation (2017M621129), by the Fundamental Research Funds for the Central Universities (DUT16RC(3)119), and by the US NSF grant CCF 1525904.

I. Introduction

A. Motivation

Heterogeneous cellular networks (HCNs) are envisioned as a promising approach to address the challenge of the explosive mobile data traffic growth and universal seamless coverage through deploying macro-, pico-, and femto-base stations (BSs) [2]. Due to the load disparity between the macro and small cells, it is desirable to offload users to small cells via flexible cell association and proper spectrum allocation. As a commonly used spectrum allocation scheme, spectrum partitioning has its practical utility since future networks are definitely fusions of multi-standard and multi-band networks. Hence different types of wireless access points (with different ratio technologies) are quite likely to operate in non-overlapping frequency bands [3, Chap. 5.2]. It has been established that these techniques are strongly coupled and directly influence the user-perceived rate [4–6]. To efficiently evaluate these techniques in HCNs, stochastic geometry is a powerful mathematical and statistical tool due to its capability of capturing the irregularity and variability of the node configurations in real networks and providing theoretical insights. However, the current analysis using stochastic geometry for the HCNs mostly focuses on the typical user by *spatial averaging*, i.e., the evaluation of a certain expectation over the point processes modeling all tiers of BSs.

While this expected value is certainly important, it does not reflect the performance variation among the individual users in the same tier or different tiers and how such variation is affected by offloading and resource allocation strategies. For example, Fig. 1 compares the distributions of the success probability $\mathbb{P}(\mathrm{SINR} > \theta \mid \Phi)$—the complementary cumulative distribution (CCDF) of the signal-to-interference-plus-noise ratio (SINR) conditioning on the BS point processes Φ—among users in each tier and the overall two-tier HCN with different biasing factors and transmit powers. It is shown that the overall distribution of the success probability in each case (i.e., averaging over tier 1 and 2) is almost the same while the per-tier success probability distribution differs greatly. This indicates that sometimes a macroscopic quantity by averaging over all the point processes conceals the actual performance of individual users and its variations influenced by the load balancing and resource partitioning. It is even worse when analyzing the *user-perceived rate*, defined as $T = W_{\mathrm{u}} \log(1 + \mathrm{SINR})$, since the load distribution among cells and tiers that affect the per-user bandwidth W_{u} is also averaged. The above discussions indicate

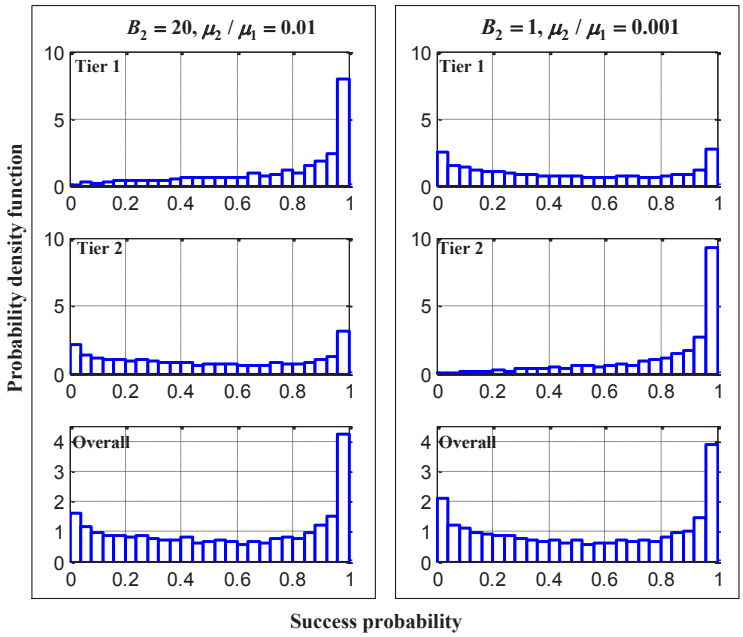

Fig. 1. The histogram of the empirical probability density function of the success probability for two-tier Poisson HCNs with spectrum partitioning, considering the power path loss law with Rayleigh fading and strongest-BS association (on biased average received power), where tier 1 density $\lambda_1 = \frac{1}{\pi 200^2}$, tier 2 density $\lambda_2 = 10\lambda_1$, path loss exponent $\alpha_1 = \alpha_2 = 4$, biasing factor $B_1 = 1$, tier 1 transmit power $\mu_1 = 46\,\mathrm{dBm}$, and SIR threshold $\theta = 2$.

that the average performance can represent neither that of users with good quality of service (QoS) nor that of users with bad QoS. Hence it is critical to deeply explore how the existing resource allocation and load balancing schemes affect the performance of individual users. This is achieved using new fine-grained performance metrics that can directly capture individual users' performance for HCNs with joint offloading and resource partitioning.

B. Related Work

Network heterogeneity and densification have been dominant themes during the ongoing evolution of 5G in response to the increasing demand for high-quality services. This emerging infrastructure, however, renders the conventional grid model unsuitable, especially for the small cells (micro, pico, femto) which are likely to be deployed opportunistically and irregularly. Recently, an increasingly popular approach is to use the homogeneous independent Poisson (HIP) model [7] from stochastic geometry to capture the irregular network topology of HCNs [4, 8, 9]. Since the concept of biased user association has been proposed by 3GPP in Release

10 [10] to cope with the load imbalance issue, the effect of biased user association was widely investigated in the context of multi-tier downlink HetNets with the aid of stochastic geometry using numerical evaluation techniques [4, 8]. However, owing to the artificial increase of users' received power from the small-cell BSs, the offloaded users are actually forced to access the BSs that are not the strongest (in terms of the received power). This implies that the strongest BS is an interferer. Thus, the offloaded users have lower SINRs than they would have with a conventional RSS-based association rule. To solve this problem, several interference mitigation schemes based on resource partitioning have been proposed and analyzed in conjunction with the biased user association [5, 6, 11, 12].

Although the aforementioned works presented some analytical results for the typical user in HCNs with biased user association or resource partitioning, none of them unraveled how the biasing and partitioning will influence the performance of individual users, which is a critical and unique problem in HCNs. Recently, the meta distribution is formulated and used for evaluating the performance of individual users/links in Poisson bipolar and cellular networks [13]. It has been shown that the SIR meta distribution provides a much sharper version of the SIR performance than the average success probability commonly evaluated at the typical link. Since then, the meta distribution has been applied to analyze the performance of D2D communication [14, 15], power control scheme [16], millimeter-wave communication [15] and coordinated multi-point transmission (CoMP) [17] in various types of wireless networks. However, these studies merely concentrate on the homogeneous (or, equivalently, single-tier) networks. Only [18] investigated the SIR meta distribution in HCNs with cell range expansion, but it did not consider the load on the BS which is critical for the user-perceived rate and also provides a view of resource allocation. It is intuitive that the SIR performance cannot reflect the actual experience of the service, e.g., the throughput can be very low at peak times due to congestion even with good signal strength. To this end, an investigation that not only studies the microscopic quantities but also reflects the intricate relationship among the user-perceived rate, the load, the biased value as well as the resource partitioning schemes is required to give insights on offloading and spectrum allocation in HCNs. This is the goal of this paper.

C. Contributions

In this paper, we focus on a fine-grained analysis for a multi-tier HCN with joint spectrum allocation and offloading, expecting to get deep insight into the impacts of heterogeneity, resource coordination, user association, etc., on the performance of individual users. Each tier of BSs is modeled by an independent Poisson point process (PPP) and differs in transmit power, path loss exponent, and density. The users are modeled by another independent PPP, and the biased user association is assumed. A spectrum allocation approach is considered where the offloaded users are allocated to a reserved frequency band so as to avoid the severe SINR degradation.

Specifically, we first present a general framework for the meta distribution analysis in terms of both the SINR and the user perceived rate in HCNs under the considered biased user association and spectrum allocation scheme. Based on the general framework, we derive the overall and per-tier moments of the conditional SINR and rate distributions given the point processes. With them, we provide analytical expressions for the exact meta distribution for the two performance metrics. In particular, for each tier, we further divide the users into two types, i.e., *offloaded* and *unoffloaded users*, and analyze their corresponding performance. Secondly, to provide new design guidelines for offloading and resource utilization in HCNs, we show the following:

- Comparing the performance of offloaded and unoffloaded users, load balancing is quite effective in improving the unoffloaded user performance, while its effect on the performance degradation for the offloaded users can be alleviated through the resource partitioning.
- Comparing the per-tier and the overall network performance, the per-tier performance can be quite different from the overall performance. The tier that dominates the overall performance highly depends on the per-tier association probability.
- Comparing the performance of different resource allocation schemes, the adopted scheme has obvious advantages in both the overall and the offloaded user performance and only a slight disadvantage in the unoffloaded user performance compared with the spectrum sharing and the spectrum partitioning. The results fully demonstrate the importance of balancing the inter-tier interference and the resource utilization when designing the resource allocation scheme.

In summary, the theoretical results lead to deep insights for the intricate relationships among the biasing factor, the spectrum allocation strategy and the performance of individual users that

are offloaded or unoffloaded as well as the performance of individual users that are in the same tier or different tiers.

II. System Model

A. Network Model

We consider a downlink HCN model consisting of K independent network tiers, where the BSs in the k-th tier are spatially distributed according to a homogeneous Poisson point process (PPP) Φ_k with density λ_k, $k = 1, 2, \ldots, K$ and fixed transmit power μ_k. We denote by $\Phi = \bigcup_{k=1}^{K} \Phi_k$ the locations of all BSs in the network. The locations of the users are modeled as another independent homogeneous PPP Φ_{u} with density λ_{u}. The channel gain between the transmitter and receiver is modeled by the large-scale path loss and the small-scale fading. A deterministic path loss function $\ell_k(r) = r^{-\alpha_k}$ is adopted, where r is the distance between the transmitter and the receiver, and α_k is the path loss exponent in the k-th tier. The small-scale fading coefficient associated with node $x \in \Phi$ is denoted by h_x, which is an exponential random variable with $\mathbb{E}(h_x) = 1$ (Rayleigh fading), and all h_x are mutually independent and also independent of Φ and Φ_{u}. The additive noise power is σ^2.

B. User Association and Spectrum Allocation

Each user is assumed to be associated with the BS that offers the strongest biased average received power. We assume a user located at the origin in the process $\Phi_{\mathrm{u}} \cup \{o\}$, which, due to Slivnyak's theorem [19, Thm. 8.10], becomes the typical user under expectation over the PPP. Denoting by Z_i the distance between the typical user and the nearest BS in the i-th tier and by B_i the association bias for the i-th tier, the serving tier, i.e., the tier that the serving BS of the typical user belongs to, is given by

$$k = \arg\max_{i \in [K]} \mu_i B_i Z_i^{-\alpha_i}, \tag{1}$$

where $[K] \triangleq \{1, 2, \ldots, K\}$. In such way, users are offloaded to the tiers with larger association bias. Without loss of generality, it is assumed that $B_i \leq B_j$ if $i < j$. Thus, if the typical user u_0 is served by a BS from tier k, it belongs to the following two user subsets

$$u_0 \in \begin{cases} \mathcal{U}_k^{\mathrm{u}} & \text{if } \mu_k Z_k^{-\alpha_k} \geq \mu_i Z_i^{-\alpha_i}, i \leq k \text{ and } \mu_k B_k Z_k^{-\alpha_k} \geq \mu_i B_i Z_i^{-\alpha_i}, i > k \\ \mathcal{U}_k^{\mathrm{o}} & \text{otherwise,} \end{cases} \tag{2}$$

where $\mathcal{U}_k^{\mathrm{u}}$ is the set of unoffloaded users for tier k and $\mathcal{U}_k^{\mathrm{o}}$ is the set of offloaded users from other tiers to tier k. Then, all the users associated with tier k are $\mathcal{U}_k = \mathcal{U}_k^{\mathrm{u}} \cup \mathcal{U}_k^{\mathrm{o}}$. It should be noted that tier 1 only has unoffloaded users because it has the smallest association biasing factor. For notational convenience, we define $\delta_k \triangleq 2/\alpha_k$, $\hat{\delta}_{ik} \triangleq \delta_i/\delta_k$ and

$$\hat{\lambda}_{ik} \triangleq \frac{\lambda_i}{\lambda_k}, \quad \hat{B}_{ik} \triangleq \frac{B_i}{B_k}, \quad \hat{\mu}_{ik} \triangleq \frac{\mu_i}{\mu_k}, \quad \hat{\alpha}_{ik} \triangleq \frac{\alpha_i}{\alpha_k}, \tag{3}$$

which characterize the density ratio, the biasing factor ratio, the transmit power ratio, and the path loss exponent ratio, respectively.

Since offloading forces those offloaded users to be associated with the BSs that are actually not the strongest owing to the added bias, it reduces their SINR performance [18]. To alleviate this negative effect, we consider an interference mitigation scheme based on spectrum partitioning, where a fraction η_1 of the frequency resources are shared among all tiers for the unoffloaded users, and the remaining resources are partitioned into $K-1$ fractions for the offloaded users of tier $k = 2, \ldots, K$, to avoid inter-tier interference for these users. Hence, the total bandwidth W is divided into K parts, where η_1 is the shared fraction for all the unoffloaded users in all tiers and η_k for $k > 1$ is the reserved fraction for the k-th tier offloaded users and $\sum\limits_{k\in[K]} \eta_k = 1$, $\eta_k > 0$. For example, in a three-tier HCN ($K = 3$) with $\eta_1 = 0.5$, $\eta_2 = 0.3$ and $\eta_3 = 0.2$, the total bandwidth is divided into three parts with 50% of the bandwidth allocated to the unoffloaded users in all the three tiers, 30% for the users offloaded to tier 2, and 20% for the users offloaded to tier 3. In each cell, transmissions are orthogonal and all users are served concurrently by dividing the resources equally between them.

C. SINR and Rate Analysis

Conditioning on that the typical user is served by the k-th tier, the corresponding received SINR, denoted as SINR_k, is given by

$$\mathrm{SINR}_k = \begin{cases} \dfrac{\mu_k \ell_k(Z_k) h_{x_k}}{\sum\limits_{x\in\Phi_k^!} \mu_k \ell_k(|x|) h_x + \sum\limits_{i\in[K]^!} \sum\limits_{x\in\Phi_i} \mu_i \ell_i(|x|) h_x + \sigma^2} & \text{if } u_0 \in \mathcal{U}_k^{\mathrm{u}}, \\ \dfrac{\mu_k \ell_k(Z_k) h_{x_k}}{\sum\limits_{x\in\Phi_k^!} \mu_k \ell_k(|x|) h_x + \sigma^2} & \text{if } u_0 \in \mathcal{U}_k^{\mathrm{o}}, \end{cases} \tag{4}$$

where x_k denotes the serving BS from tier k, $Z_k = |x_k|$, $\Phi_k^! = \Phi_k \setminus \{x_k\}$, and $[K]^! = [K] \setminus \{k\}$.

Letting N_k^{u} and N_k^{o} denote the numbers of the unoffloaded and offloaded users served by the tagged BS (the BS serving the typical user) in tier k, respectively, the user-perceived rate for

the typical user is given as

$$T_k = \begin{cases} \frac{\eta_1 W}{N_k^{\mathrm{u}}} \log(1+\mathrm{SINR}_k) & \text{if } u_0 \in \mathcal{U}_k^{\mathrm{u}}, \\ \frac{\eta_k W}{N_k^{\mathrm{o}}} \log(1+\mathrm{SINR}_k) & \text{if } u_0 \in \mathcal{U}_k^{\mathrm{o}}, \end{cases} \tag{5}$$

which is related to the per-user available resource, the load in the typical cell and the received SINR.

D. Meta Distribution

The SINR and the data rate are two fundamental performance metrics for users in cellular networks, and we focus on the fine-grained characterization of these two metrics. Letting T be the (random) data rate of the typical user, the meta distributions are the CCDFs of the random variables

$$\begin{aligned} P_{\mathrm{s}}(\theta) &\triangleq \mathbb{P}(\mathrm{SINR} > \theta \mid \Phi), \\ P_{\mathrm{c}}(\tau) &\triangleq \mathbb{P}(T > \tau \mid \Phi), \end{aligned} \tag{6}$$

where θ and τ are thresholds for the SINR and rate, respectively, and the conditional probability is taken over all the other random effects (such as the fading, the channel access scheme, etc.) given the BS point process, and the randomness of (6) is due to the dependence on Φ. Therefore, the meta distribution is defined as

$$\bar{F}(y,x) \triangleq \mathbb{P}(P(y) > x), \quad y \in \mathbb{R}^+, \quad x \in [0,1], \tag{7}$$

where $P(y)$ is $P_{\mathrm{s}}(\theta)$ or $P_{\mathrm{c}}(\tau)$ corresponding to $y{=}\theta$ or $y{=}\tau$. Due to the ergodicity of the point process, the meta distribution can be interpreted as the fraction of links in each realization of the point process that have a SINR (or rate) greater than θ (or τ) with probability at least x.

By such a definition, the standard success probability (or rate coverage probability) is the mean of $P_{\mathrm{s}}(\theta)$ (or $P_{\mathrm{c}}(\tau)$), obtained by integrating the meta distribution (7) over $x \in [0,1]$. The standard success probability (or rate coverage probability) answers the question "Given a threshold θ (or τ), what fraction of users can achieve the required SINR (or rate) in each realization of the point process?" without notion of reliability, and the set of users that meet the SINR (or rate) threshold changes over time. As a result, it allows no statement about individual users. Each user meets the required SINR (or rate) sometimes, and sometimes it does not, thus we have no information on how often a user meets it. The meta distribution, in contrast, answers more

TABLE I. Symbols and descriptions

Symbol	Description	Default value
K	The number of the tiers	2
Φ_k, λ_k	The PPP of tier k and density	$\lambda_1 = \frac{1}{\pi 200^2}$, $\lambda_2 = \frac{5}{\pi 200^2}$
μ_k	The transmit power of the BS in tier k	$\mu_1 = 46$ dBm, $\mu_2 = 26$ dBm
α_k	The path loss exponent for tier k	$\alpha_1 = \alpha_2 = 4$
η_k	The resource fraction of tier k	N/A
B_k	The bias factor of tier k	$B_1 = 1$, $B_2 = 10$
θ, τ	The SINR threshold, rate threshold	0 dB, 1 Mbps
W	The total bandwidth	10 MHz
σ^2	The noise power	0
$\lambda_{\rm u}$	The density of users	$\lambda_{\rm u} = \frac{50}{\pi 200^2}$
$\mathcal{U}_k$, $\mathcal{U}_k^{\rm u}$, $\mathcal{U}_k^{\rm o}$	The total/unoffloaded/offloaded user set of tier k	N/A
M_b, S_b	The b-th moments of $P_{\rm s}(\theta)$, $P_{\rm c}(\tau)$	N/A

detailed questions such as "Given a reliability threshold x and an SINR (or rate) threshold θ (or τ), what fraction of users achieves such reliability in each realization of the point process?". Here the set of users that achieve θ (or τ) with probability x is constant over time.

The main symbols and parameters are summarized in Table I, and default values are given where applicable.

III. Auxiliary Results

In this section, we give some auxiliary results that are essential for the meta distribution analyses of the SINR and rate in the next section, including the per-tier association probability and load distribution as well as the statistical distance of the serving BS. The first lemma provides the per-tier association probability of the typical user and further gives the per-tier association probability if the typical user is offloaded and unoffloaded.

Lemma 1. *The probabilities of $u_0 \in \mathcal{U}_k$, $u_0 \in \mathcal{U}_k^{\rm u}$ and $u_0 \in \mathcal{U}_k^{\rm o}$ are given, respectively, as*

$$A_k = \pi \lambda_k \int_0^\infty \exp\Big(- \sum_{i \in [K]} \pi \lambda_i (\hat{\mu}_{ik} \hat{B}_{ik})^{\delta_i} r^{\hat{\delta}_{ik}} \Big) {\rm d}r, \tag{8}$$

$$A_k^{\mathrm{u}} = \pi\lambda_k \int_0^{\infty} \exp\Big(- \sum_{i\le k} \pi\lambda_i \hat{\mu}_{ik}^{\delta_i} r^{\hat{\delta}_{ik}} - \sum_{i>k} \pi\lambda_i (\hat{\mu}_{ik}\hat{B}_{ik})^{\delta_i} r^{\hat{\delta}_{ik}}\Big)\mathrm{d}r, \tag{9}$$

and $A_k^{\mathrm{o}} = A_k - A_k^{\mathrm{u}}$.

Proof: See Appendix A.

Since the desired signal strength depends on the distance between the typical user and its serving BS, the following lemma gives the statistical distribution of this contact distance [19].

Lemma 2. *Given that the typical user is associated with a BS from the k-th tier, the probability density function (PDF) of the distance Z_k between the typical user and its serving BS is*

$$f_{Z_k|u_0\in\mathcal{U}_k}(r) = \frac{2\pi\lambda_k r}{A_k} \exp\Big(- \sum_{i\in[K]} \pi\lambda_i (\hat{\mu}_{ik}\hat{B}_{ik})^{\delta_i} r^{2\hat{\delta}_{ik}}\Big). \tag{10}$$

Furthermore, if the typical user is an unoffloaded user for tier k, the PDF is

$$f_{Z_k|u_0\in\mathcal{U}_k^{\mathrm{u}}}(r) = \frac{2\pi\lambda_k r}{A_k^{\mathrm{u}}} \exp\Big(- \sum_{i\le k} \pi\lambda_i \hat{\mu}_{ik}^{\delta_i} r^{2\hat{\delta}_{ik}} - \sum_{i>k} \pi\lambda_i (\hat{\mu}_{ik}\hat{B}_{ik})^{\delta_i} r^{2\hat{\delta}_{ik}}\Big), \tag{11}$$

whereas if the typical user is an offloaded user for tier k, the PDF is

$$\begin{aligned} f_{Z_k|u_0\in\mathcal{U}_k^{\mathrm{o}}}(r) = \frac{2\pi\lambda_k r}{A_k^{\mathrm{o}}} \Bigg[& \exp\Big(- \sum_{i\in[K]} \pi\lambda_i (\hat{\mu}_{ik}\hat{B}_{ik})^{\delta_i} r^{2\hat{\delta}_{ik}}\Big) \\ & - \exp\Big(- \sum_{i\le k} \pi\lambda_i \hat{\mu}_{ik}^{\delta_i} r^{2\hat{\delta}_{ik}} - \sum_{i>k} \pi\lambda_i (\hat{\mu}_{ik}\hat{B}_{ik})^{\delta_i} r^{2\hat{\delta}_{ik}}\Big)\Bigg]. \end{aligned} \tag{12}$$

Proof: See Appendix B.

IV. The Meta Distributions for HCNs

Since a direct calculation of the meta distributions seems infeasible, we will derive an exact analytical expression through the moments $M_b(\theta) \triangleq \mathbb{E}\left[P_{\mathrm{s}}(\theta)^b\right]$ and $S_b(\tau) \triangleq \mathbb{E}\left[P_{\mathrm{c}}(\tau)^b\right]$. Therefore, in this section, we first derive the per-tier and overall moments of the conditional SINR and rate distributions, respectively, and then we give the meta distributions of the SINR and rate for HCNs.

We define $F_b(\alpha,\theta) \triangleq 1 + 2\int_0^{\infty}(1 - \frac{1}{(1+\theta z^{\alpha})^b})z^{-3}\mathrm{d}z$, which can be expressed in terms of the Gaussian hypergeometric function ${}_2F_1(\cdot)$ as

$$F_b(\alpha,\theta) = {}_2F_1(b, -\delta; 1-\delta, -\theta). \tag{13}$$

The moments of the conditional success probability for a interference-limited homogeneous Poisson cellular network (i.e., $\sigma^2 = 0$) can be expressed as $M_b(\theta) = 1/F_b(\alpha, \theta)$ [13]. The same expression holds for the HIP model without biasing or offloading [18].

A. Moments of the Conditional Success Probability

The following theorem gives the per-tier moments of the conditional success probability.

Theorem 1. *Given that the typical user is served by tier k, the moments of the conditional success probability for $u_0 \in \mathcal{U}_k^{\mathrm{u}}$ and $u_0 \in \mathcal{U}_k^{\mathrm{o}}$ are, respectively, given as*

$$M_{b|k}^{\mathrm{u}}(\theta) = \frac{\pi\lambda_k}{A_k^{\mathrm{u}}} \int_0^\infty e^{-\frac{b\sigma^2\theta}{\mu_k} r^{\frac{\alpha_k}{2}}} \exp\Big(-\pi \sum_{i\le k} \lambda_i \hat{\mu}_{ik}^{\delta_i} r^{\hat{\delta}_{ik}} F_b(\alpha_i, \theta) - \pi \sum_{i>k} \lambda_i (\hat{\mu}_{ik}\hat{B}_{ik})^{\delta_i} r^{\hat{\delta}_{ik}} F_b\big(\alpha_i, \theta \hat{B}_{ik}^{-1}\big)\Big) \mathrm{d}r, \tag{14}$$

$$M_{b|k}^{\mathrm{o}}(\theta) = \frac{\pi\lambda_k}{A_k^{\mathrm{o}}} \int_0^\infty e^{-\frac{b\sigma^2\theta}{\mu_k} r^{\frac{\alpha_k}{2}}} \exp\Big(-\sum_{i>k} \pi\lambda_i (\hat{\mu}_{ik}\hat{B}_{ik})^{\delta_i} r^{\hat{\delta}_{ik}} - \pi\lambda_k F_b(\alpha_k, \theta) r \Big) \times \Big[\exp\Big(-\sum_{i<k} \pi\lambda_i (\hat{\mu}_{ik}\hat{B}_{ik})^{\delta_i} r^{\hat{\delta}_{ik}} \Big) - \exp\Big(-\sum_{i<k} \pi\lambda_i \hat{\mu}_{ik}^{\delta_i} r^{\hat{\delta}_{ik}} \Big) \Big] \mathrm{d}r, \tag{15}$$

and thus the per-tier moments of the SINR are $M_{b|k}(\theta) = \frac{1}{A_k}\big(A_k^{\mathrm{u}} M_{b|k}^{\mathrm{u}}(\theta) + A_k^{\mathrm{o}} M_{b|k}^{\mathrm{o}}(\theta)\big)$, $b \in \mathbb{C}$.

Proof: See Appendix C.

When the path loss exponents are identical, i.e., $\alpha_k = \alpha$, $k \in [K]$, the moments in Thm. 1 can be approximated to a simpler form that does not involve integrals using [21, Eq. (5) and (13)]. Furthermore, when we consider an interference-limited network with identical path loss exponent, i.e., $\sigma^2 = 0$, and $\alpha_k = \alpha$, $k \in [K]$, the exact expressions in Thm. 1 simplify to

$$M_{b|k}^{\mathrm{u}}(\theta) = \frac{\sum_{i\le k} \hat{\lambda}_{ik} \hat{\mu}_{ik}^{\delta} + \sum_{i>k} \hat{\lambda}_{ik} (\hat{B}_{ik}\hat{\mu}_{ik})^{\delta}}{\sum_{i\le k} \hat{\lambda}_{ik} \hat{\mu}_{ik}^{\delta} F_b(\alpha, \theta) + \sum_{i>k} \hat{\lambda}_{ik} (\hat{B}_{ik}\hat{\mu}_{ik})^{\delta} F_b(\alpha, \theta \hat{B}_{ik}^{-1})}, \tag{16}$$

$$M_{b|k}^{\mathrm{o}}(\theta) = \frac{\Big(\sum_{i\le k} \hat{\lambda}_{ik} \hat{\mu}_{ik}^{\delta} + \sum_{i>k} \hat{\lambda}_{ik} (\hat{B}_{ik}\hat{\mu}_{ik})^{\delta} \Big) \sum_{i\in[K]} \hat{\lambda}_{ik} (\hat{B}_{ik}\hat{\mu}_{ik})^{\delta}}{\Big(\sum_{i<k} \hat{\lambda}_{ik} \hat{\mu}_{ik}^{\delta} + \sum_{i>k} \hat{\lambda}_{ik} (\hat{B}_{ik}\hat{\mu}_{ik})^{\delta} + F_b(\alpha, \theta) \Big) \Big(\sum_{i\in[K]^!} \hat{\lambda}_{ik} (\hat{B}_{ik}\hat{\mu}_{ik})^{\delta} + F_b(\alpha, \theta) \Big)}. \tag{17}$$

With the per-tier moments of the conditional success probability, the overall moments follow as

$$M_b(\theta) = \sum_{k\in[K]} A_k^{\mathrm{u}} M_{b|k}^{\mathrm{u}}(\theta) + A_k^{\mathrm{o}} M_{b|k}^{\mathrm{o}}(\theta). \tag{18}$$

According to the Gil-Pelaez theorem, the meta distribution of the SINR is given by [13]

$$\bar{F}_{P_{\mathrm{s}}(\theta)}(x) = \frac{1}{2} + \frac{1}{\pi}\int_0^\infty \frac{\Im\left(e^{-jt\log x}\mathcal{M}_{jt}\right)}{t}\mathrm{d}t \tag{19}$$

where $\mathcal{M}_{jt}$ can be $M_{jt|k}^{\mathrm{u}}$ in (14), $M_{jt|k}^{\mathrm{o}}$ in (15) or M_{jt} in (18) corresponding to the unoffloaded/offloaded per-tier and overall distributions of the conditional success probability, respectively, $j \triangleq \sqrt{-1}$, $\Im(z)$ and $\Re(z)$ are the imaginary and real parts of $z \in \mathbb{C}$. Though the exact meta distribution has a complex form, the computational complexity can be significantly reduced via efficient calculation methods [20, 21].

B. Moments of the Conditional Rate Coverage

The conditional rate coverage is defined as the rate coverage probability of the typical user conditioning on the BS point processes, i.e., $P_{\mathrm{c}}(\tau) \triangleq \mathbb{P}(T > \tau \mid \Phi)$ in (6). Since the user-perceived rate depends on the number of users concurrently served by a BS, the rate meta distribution involves its corresponding probability mass functions (PMFs). To express the PMFs conveniently, we define

$$U_{n,k}(x) \triangleq \frac{1}{\Gamma(n)}\left(\frac{\lambda_{\mathrm{u}} x}{3.5\lambda_k}\right)^{n-1}\frac{\Gamma(3.5+n)}{\Gamma(4.5)}\left(1+\frac{\lambda_{\mathrm{u}} x}{3.5\lambda_k}\right)^{-3.5-n}, \quad n \geq 1. \tag{20}$$

where the relationship between $U_{n,k}(x)$ and the PMFs is given in the proof of Thm. 2. According to Thm. 1, we derive the per-tier moments of the conditional rate coverage probability as follows.

Theorem 2. *Given that the typical user is served by tier k, the moments of the conditional rate coverage probability for $u_0 \in \mathcal{U}_k^{\mathrm{u}}$ and $u_0 \in \mathcal{U}_k^{\mathrm{o}}$ are, respectively, given as*

$$\begin{aligned} S_{b|k}^{\mathrm{u}}(\tau) &\approx \sum_{n=1}^{\infty} U_{n,k}(A_k^{\mathrm{u}}) M_{b|k}^{\mathrm{u}}\big(2^{\frac{n\tau}{\eta_1 W}} - 1\big), \\ S_{b|k}^{\mathrm{o}}(\tau) &\approx \sum_{n=1}^{\infty} U_{n,k}(A_k^{\mathrm{o}}) M_{b|k}^{\mathrm{o}}\big(2^{\frac{n\tau}{\eta_k W}} - 1\big), \end{aligned} \tag{21}$$

and thus the per-tier moments of the rate coverage probability for $u_0 \in \mathcal{U}_k$ are $S_{b|k}(\tau) = \frac{1}{A_k}\big(A_k^{\mathrm{u}} S_{b|k}^{\mathrm{u}}(\tau) + A_k^{\mathrm{o}} S_{b|k}^{\mathrm{o}}(\tau)\big)$, $b \in \mathbb{C}$.

Proof: Given Φ and the condition that the typical user is an unoffloaded user for tier k, the conditional rate coverage probability is expressed as

$$P_{\mathrm{c},k}(\tau) = \mathbb{P}(T_k > \tau \mid \Phi, u_0 \in \mathcal{U}_k^{\mathrm{u}}). \tag{22}$$

Therefore, the moments of the conditional rate coverage probability for the unoffloaded users in tier k are

$$\begin{aligned} S_{b|k}^{\mathrm{u}}(\tau) &= \mathbb{E}\left[\mathbb{P}\Big(T_k>\tau \mid u_0 \in \mathcal{U}_k^{\mathrm{u}}, \Phi\Big)^b\right] \\ &= \mathbb{E}_{N_k^{\mathrm{u}}}\left\{\mathbb{E}\left[\mathbb{P}\left(T_k>\tau \mid u_0 \in \mathcal{U}_k^{\mathrm{u}}, \Phi, N_k^{\mathrm{u}}\right)^b\right]\right\} \\ &\overset{(a)}{=} \sum_{n=1}^{\infty} p_{n,k}^{\mathrm{u}} \underbrace{\mathbb{E}\left[\mathbb{P}\Big(\mathrm{SINR}_k>2^{\frac{n\tau}{\eta_1 W}}-1 \mid u_0 \in \mathcal{U}_k^{\mathrm{u}}, \Phi\Big)^b\right]}_{\mathcal{X}} \\ &= \sum_{n=1}^{\infty} p_{n,k}^{\mathrm{u}} M_{b|k}^{\mathrm{u}}\big(2^{\frac{n\tau}{\eta_1 W}}-1\big), \end{aligned} \tag{23}$$

where (a) follows that N_k^{u} and SINR_k are assumed to be independent[1] and $\mathcal{X} = M_{b|k}^{\mathrm{u}}(\theta)$ with $\theta = 2^{\frac{n\tau}{\eta_k W}}-1$ according to (45). $p_{n,k}^{\mathrm{u}} = \mathbb{P}(N_k^u = n)$ is given as follows.

Letting $N_{o,k}^{\mathrm{u}}$ be the number of the unoffloaded users served by the tagged BS except for the typical user, i.e., $N_k^{\mathrm{u}} = N_{o,k}^{\mathrm{u}} + 1$, we have $\mathbb{P}(N_k^{\mathrm{u}} = n) = \mathbb{P}(N_{o,k}^{\mathrm{u}} = n-1)$. As in [4], the probability generating function (PGF) of $N_{o,k}^{\mathrm{u}}$ is approximated by

$$G_{N_{o,k}^{\mathrm{u}}}(z) \approx \left(1 - \frac{\lambda_{\mathrm{u}} A_k^{\mathrm{u}}(z-1)}{3.5\lambda_k}\right)^{-4.5}. \tag{24}$$

Thus, we have

$$\begin{aligned} \mathbb{P}(N_k^{\mathrm{u}}=n) &= \frac{1}{(n-1)!} G_{N_{o,k}^{\mathrm{u}}}^{(n-1)}(0) \\ &\approx \frac{1}{\Gamma(n)}\left(\frac{\lambda_{\mathrm{u}} A_k^{\mathrm{u}}}{3.5\lambda_k}\right)^{n-1} \frac{\Gamma(3.5+n)}{\Gamma(4.5)}\left(1+\frac{\lambda_{\mathrm{u}} A_k^{\mathrm{u}}}{3.5\lambda_k}\right)^{-3.5-n} = U_{n,k}(A_k^{\mathrm{u}}). \end{aligned} \tag{25}$$

By substituting (25) into (23), $S_{b|k}^{\mathrm{u}}(\tau)$ is obtained.

The moments of the conditional rate coverage probability for the offloaded users can be obtained in a similar way. Thus, according to the total probability law, we obtain the per-tier

[1]The Pearson's correlation coefficient is less than 0.04 in all cases studied by simulation.

moments of the conditional rate coverage probability, i.e., $S_{b|k}(\tau) = \frac{1}{A_k}\big(A_k^{\mathrm{u}} S_{b|k}^{\mathrm{u}}(\tau) + A_k^{\mathrm{o}} S_{b|k}^{\mathrm{o}}(\tau)\big)$. ■

The following corollary gives the overall moments of the conditional rate coverage for HCNs.

Corollary 1. *The moments S_b of the conditional rate coverage probability are*

$$S_b(\tau) = \sum_{k\in[K]} \sum_{n=1}^{\infty} U_{n,k}(A_k^{\mathrm{u}}) M_{b,k}^{\mathrm{u}}\big(2^{\frac{n\tau}{\eta_k W}} - 1\big) + U_{n,k}(A_k^{\mathrm{o}}) M_{b,k}^{\mathrm{o}}\big(2^{\frac{n\tau}{\eta_k W}} - 1\big),\ b \in \mathbb{C}, \tag{26}$$

where

$$\begin{aligned} M_{b,k}^{\mathrm{u}}(\theta) = \int_0^{\infty} \exp\Bigg(& - \frac{b\sigma^2\theta r^{\frac{\alpha_k}{2}}}{\mu_k(\pi\lambda_k)^{\frac{\alpha_k}{2}}} - \sum_{i\le k} \frac{\pi\lambda_i \hat{\mu}_{ik}^{\delta_i}}{(\pi\lambda_k)^{\frac{\alpha_k}{\alpha_i}}} r^{\frac{\alpha_k}{\alpha_i}} F_b(\alpha_i,\theta) \\ & - \sum_{i>k} \frac{\pi\lambda_i(\hat{\mu}_{ik}\hat{B}_{ik})^{\delta_i}}{(\pi\lambda_k)^{\frac{\alpha_k}{\alpha_i}}} r^{\frac{\alpha_k}{\alpha_i}} F_b\big(\alpha_i, \theta\hat{B}_{ik}^{-1}\big)\Bigg)\mathrm{d}r, \end{aligned} \tag{27}$$

$$\begin{aligned} M_{b,k}^{\mathrm{o}}(\theta) = & \int_0^{\infty} \exp\Bigg(- \frac{b\sigma^2\theta r^{\frac{\alpha_k}{2}}}{\mu_k(\pi\lambda_k)^{\frac{\alpha_k}{2}}} - \sum_{i>k} \frac{\pi\lambda_i(\hat{\mu}_{ik}\hat{B}_{ik})^{\delta_i}}{(\pi\lambda_k)^{\frac{\alpha_k}{\alpha_i}}} r^{\frac{\alpha_k}{\alpha_i}} - F_b(\alpha_k,\theta) r\Bigg) \\ & \times\Bigg[\exp\Bigg(- \sum_{i<k} \frac{\pi\lambda_i(\hat{\mu}_{ik}\hat{B}_{ik})^{\delta_i}}{(\pi\lambda_k)^{\frac{\alpha_k}{\alpha_i}}} r^{\frac{\alpha_k}{\alpha_i}}\Bigg) - \exp\Bigg(- \sum_{i<k} \frac{\pi\lambda_i\hat{\mu}_{ik}^{\delta_i}}{(\pi\lambda_k)^{\frac{\alpha_k}{\alpha_i}}} r^{\frac{\alpha_k}{\alpha_i}}\Bigg)\Bigg]\mathrm{d}r. \end{aligned} \tag{28}$$

Proof: Given Φ, the conditional rate coverage probability of the typical overall user is

$$\begin{aligned} P_{\mathrm{c}}(\tau) &= \mathbb{P}(T > \tau \mid \Phi) \\ &= \sum_{k\in[K]} \mathbb{P}(T_k > \tau \mid \Phi)\mathbf{1}_{\{u_0\in\mathcal{U}_k|\Phi\}}, \end{aligned} \tag{29}$$

where $\mathbf{1}_{\{\cdot\}}$ is the indicator function. Then, the overall b-th moment can be expressed as

$$\begin{aligned} S_b(\tau) &= \mathbb{E}\Big[P_{\mathrm{c}}(\tau)^b\Big] \\ &= \mathbb{E}\sum_{k\in[K]}\Big(\mathbb{P}(T_k > \tau \mid \Phi)\mathbf{1}_{u_0\in\mathcal{U}_k|\Phi\}}\Big)^b \\ &= \sum_{k\in[K]} A_k \mathbb{E}\Big[\mathbb{P}(T_k > \tau, \mid u_0 \in \mathcal{U}_k, \Phi)^b\Big] \\ &= \sum_{k\in[K]} A_k^{\mathrm{u}} S_{b|k}^{\mathrm{u}}(\tau) + A_k^{\mathrm{o}} S_{b|k}^{\mathrm{o}}(\tau) \\ &= \sum_{k\in[K]} \sum_{n=1}^{\infty} U_{n,k}(A_k^{\mathrm{u}}) A_k^{\mathrm{u}} S_{b|k}^{\mathrm{u}}(\tau) + U_{n,k}(A_k^{\mathrm{o}}) A_k^{\mathrm{o}} S_{b|k}^{\mathrm{o}}(\tau). \end{aligned} \tag{30}$$

By substituting (14) and (15) into (30), we obtain (26). ■

Similar to the SINR, we can also give the meta distribution of the rate according to the Gil-Pelaez theorem by replacing $\mathcal{M}_{jt}$ with $\mathcal{S}_{jt}$ in (19), where $\mathcal{S}_{jt}$ can be $S^{\mathrm{u}}_{jt|k}$, $S^{\mathrm{o}}_{jt|k}$ in (21) or S_{jt} in (26) corresponding to the unoffloaded/offloaded per-tier and overall distributions of the conditional rate coverage probability, respectively.

C. Comparison with Other Spectrum Allocation Schemes

In this subsection, we compare our analytical results to those with the spectrum sharing and spectrum partitioning schemes to highlight the performance advantage range of each scheme. Spectrum sharing refers to the scheme where all tiers in the network share the same frequency resources (universal frequency reuse), which causes inter-tier interference; spectrum partitioning refers to the scheme where each tier in the network occupies an exclusive frequency band without any inter-tier interference. Due to the partial spectrum sharing, the adopted scheme in this paper lies in between the two extremes of spectrum sharing and the spectrum partitioning.

1) Spectrum sharing: In this scheme, the interfering signal power for the user comes from all BSs excluding the serving one, and the corresponding b-th moments of the conditional success probability and rate coverage are given in the following corollary.

Corollary 2. *For K-tier HCNs with spectrum sharing among tiers, given that the typical user is served by tier k, the moments of the conditional success probability are*

$$M^{\mathrm{s}}_{b|k}(\theta) = \frac{\pi\lambda_k}{A_k}\int_0^\infty e^{-\frac{b\sigma^2\theta}{\mu_k}r^{\frac{\alpha_k}{2}}}\exp\Big(-\pi\sum_{i\in[K]}\lambda_i(\hat{\mu}_{ik}\hat{B}_{ik})^{\delta_i}r^{\hat{\delta}_{ik}}F_b\big(\alpha_i,\theta\hat{B}_{ik}^{-1}\big)\Big)\mathrm{d}r,\ b\in\mathbb{C}, \tag{31}$$

and the moments of the conditional rate coverage probability are

$$S^{\mathrm{s}}_{b|k}(\tau) = \sum_{n=1}^{\infty}U_{n,k}(A_k)M^{\mathrm{s}}_{b|k}\big(2^{\frac{n\tau}{W}}-1\big). \tag{32}$$

The proof is omitted due to its similarity to the case of the unoffloaded users in Theorems 1 and 2. Then, the moments S^{s}_b of the conditional rate coverage probability are

$$S^{\mathrm{s}}_b(\tau) = \sum_{k\in[K]}\sum_{n=1}^{\infty}U_{n,k}(A_k)M^{\mathrm{s}}_{b,k}\big(2^{\frac{n\tau}{W}}-1\big), \tag{33}$$

where

$$M^{\mathrm{s}}_{b,k}(\theta) = \pi\lambda_k\int_0^\infty e^{-\frac{b\sigma^2\theta}{\mu_k}r^{\frac{\alpha_k}{2}}}\exp\Big(-\pi\sum_{i\in[K]}\lambda_i(\hat{\mu}_{ik}\hat{B}_{ik})^{\delta_i}r^{\hat{\delta}_{ik}}F_b\big(\alpha_i,\theta\hat{B}_{ik}^{-1}\big)\Big)\mathrm{d}r,\ b\in\mathbb{C}. \tag{34}$$

2) Spectrum Partitioning: In this scheme, the total bandwidth is partitioned into K parts and the k-th tier is allocated a fraction η_k of the total bandwidth W, where $\sum_{k=1}^{K}\eta_k = 1$, $\eta_k > 0$. The interfering signal for the user only comes from the BSs within the same tier, and the corresponding b-th moments of conditional success probability and rate coverage are given straightforwardly based on the analysis for the case of the offloaded users Theorem 1 and 2 as follows.

Corollary 3. *For K-tier HCNs with spectrum partitioning among tiers, given that the typical user is served by tier k, the moments of the conditional success probability are*

$$M^{\mathrm{p}}_{b|k}(\theta) = \frac{\pi\lambda_k}{A_k}\int_0^{\infty} e^{-\frac{b\sigma^2\theta}{\mu_k}r^{\frac{\alpha_k}{2}}}\exp\Bigg(-\sum_{i\in[K]^!}\pi\lambda_i(\hat{\mu}_{ik}\hat{B}_{ik})^{\delta_i}r^{\frac{\alpha_k}{\alpha_i}} - \pi\lambda_k F_b(\alpha_k,\theta)r\Bigg)\mathrm{d}r,\ b\in\mathbb{C}. \tag{35}$$

and the moments of the conditional rate coverage probability are

$$S^{\mathrm{p}}_{b|k}(\tau) = \sum_{n=1}^{\infty} U_{n,k}(A_k) M^{\mathrm{p}}_{b|k}\big(2^{\frac{n\tau}{\eta_k W}} - 1\big), \tag{36}$$

Then, the moments S^{p}_b of the conditional rate coverage probability are

$$S^{\mathrm{p}}_{b}(\tau) = \sum_{k\in[K]}\sum_{n=1}^{\infty} U_{n,k}(A_k) M^{\mathrm{p}}_{b,k}\big(2^{\frac{n\tau}{\eta_k W}} - 1\big), \tag{37}$$

where

$$M^{\mathrm{p}}_{b,k}(\theta) = \pi\lambda_k\int_0^{\infty} e^{-\frac{b\sigma^2\theta}{\mu_k}r^{\frac{\alpha_k}{2}}}\exp\Bigg(-\sum_{i\in[K]^!}\pi\lambda_i(\hat{\mu}_{ik}\hat{B}_{ik})^{\delta_i}r^{\frac{\alpha_k}{\alpha_i}} - \pi\lambda_k F_b(\alpha_k,\theta)r\Bigg)\mathrm{d}r,\ b\in\mathbb{C}. \tag{38}$$

V. Numerical Results

In this section, we present numerical results of various performance metrics involved in the framework in Section IV for HCNs. We consider the two-tier HCN in the following results, i.e., $K = 2$, where tier 1 and 2 correspond to the macro and pico tiers, respectively.

A. SINR Performance Trends

Fig. 2 shows the standard per-tier success probability M_1 and the variance of the conditional per-tier success probability $M_2 - M_1^2$ as a function of θ, where M_b is $M^{\mathrm{u}}_{b|k}$ or $M^{\mathrm{o}}_{b|k}$ according to the user type and the tier index. It is observed that increasing the density ratio does not affect the performance of the unoffloaded pico-cell users (PUs) because when $k = K$, (16) turns to

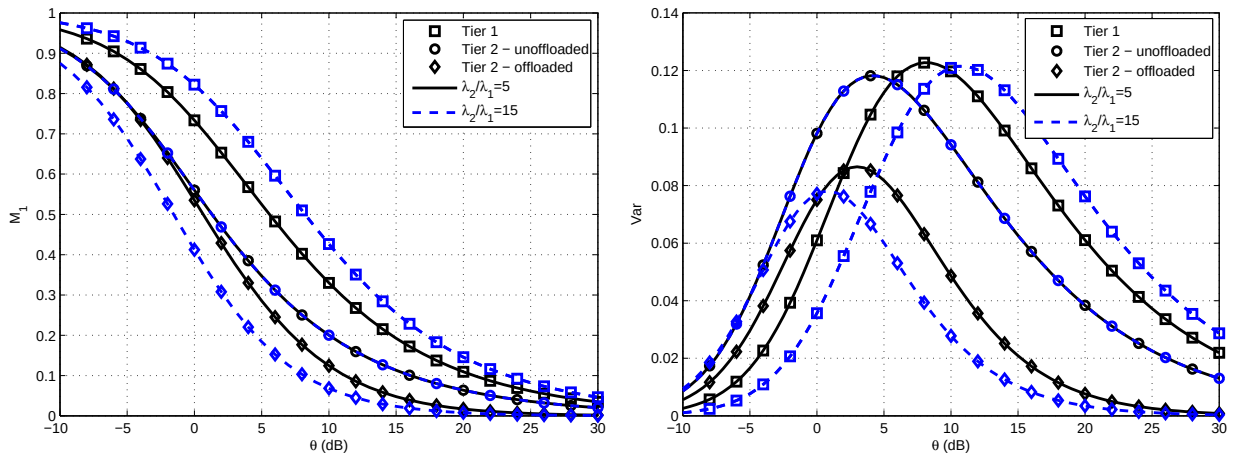

(a) The standard success probability M_1.

(b) The variance $M_2 - M_1^2$.

Fig. 2. The standard per-tier success probability and the variance for different types of users.

the homogeneous case, i.e., $M_{b|2}^{\mathrm{u}}(\theta) = 1/F_b(\alpha, \theta)$, which is independent of the node density. In contrast, it enhances the performance of macro-cell users (MUs) while it degrades that of the users offloaded from the macro to the pico tier. This indicates that increasing the density ratio motivates more users to access the pico BSs due to the closer distance but leads to an increase of the intra-tier interference, which aggravates the SINR degradation of the offloaded users. As for the variance, the density ratio mainly affects the value of θ corresponding to the maximum and the performance fluctuation of the offloaded users is smaller than that of the MUs and the unoffloaded PUs.

Fig. 3 further studies the impact of the biasing factor on the performance as in Fig. 2. Since B_2 contributes to the offloading from macro tier to pico tier, it does not affect the performance of the unoffloaded PUs but clearly improves that of MUs. As expected, the performance of the users that are offloaded from macro tier to pico tier does not experience severe SINR degradation due to the avoidance of the inter-tier interference based on spectrum partitioning. The variance demonstrates quite different trends from the mean M_1: on the one hand, for MUs, the variance significantly decreases as B_2 increases or θ decreases due to the fact that users located more close to the cell center get better and more stable SINR performance; on the other hand, influenced by the biasing factor, the performance fluctuation of PUs is in general much less than that of MUs. Moreover, there is an intersection point between the two curves of the offloaded PUs in terms

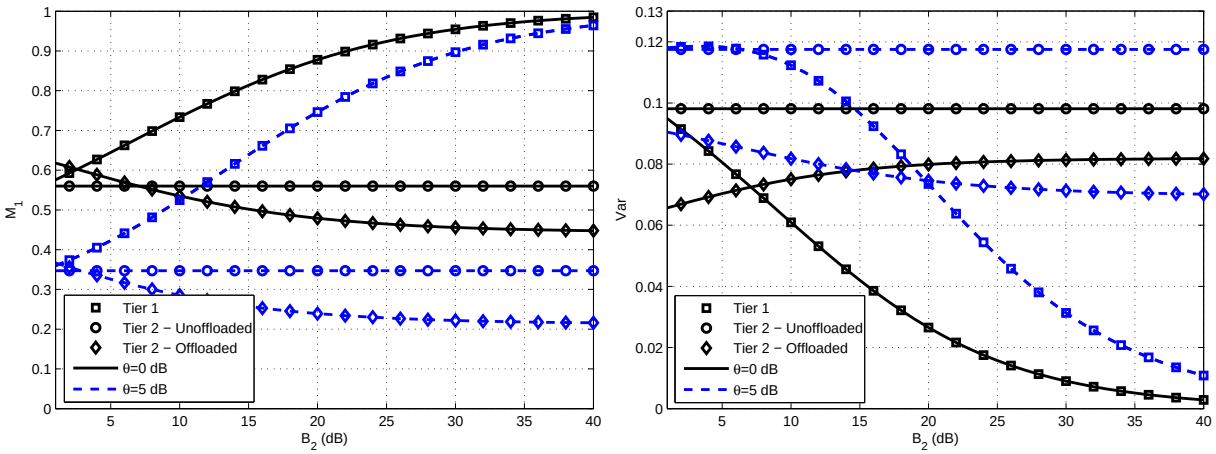

(a) The standard success probability M_1.

(b) The variance $M_2 - M_1^2$.

Fig. 3. The impact of biasing factor on the per-tier success probability and the variance for different types of users.

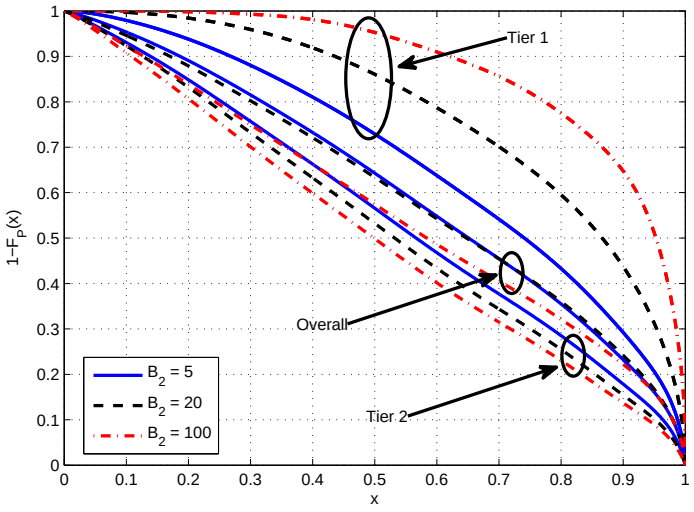

Fig. 4. The SINR meta distribution for different B_2.

of the variance, while the corresponding success probability of $\theta = 0$ dB is always higher than that of $\theta = 5$ dB, which validates the necessity of using a more refined performance metric.

Fig. 4 illustrates the per-tier and overall meta distribution of the SINR for different biasing factors. It is observed that tier 1 and tier 2 present quite different performance trends with the increase of B_2 while the overall performance is dominated by that in tier 2. Benefiting from the offloading, the performance of the individual users in tier 1 is significantly improved, e.g.,

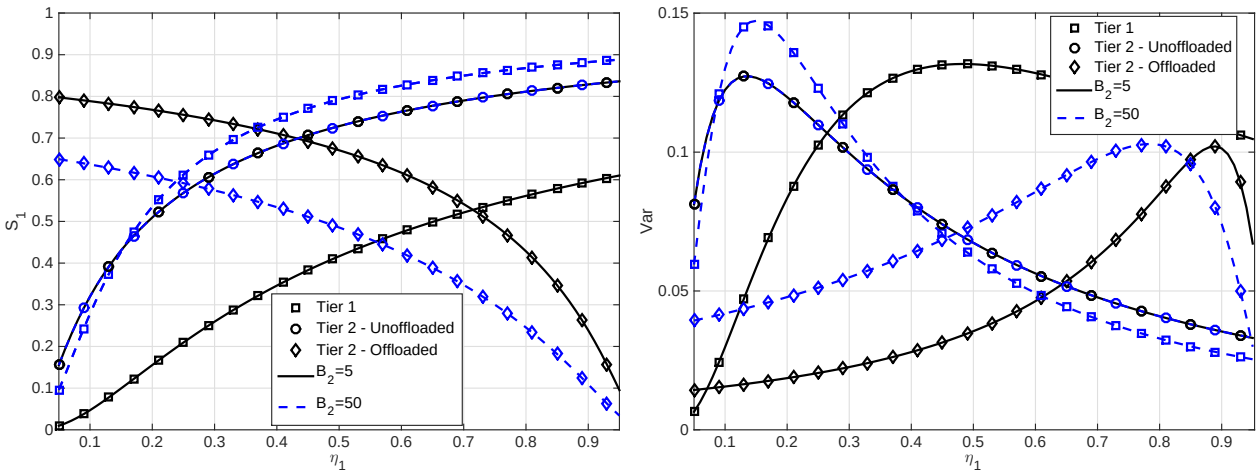

(a) The standard rate coverage probability S_1.

(b) The variance $S_2 - S_1^2$.

Fig. 5. The impact of η_1 on the rate performance for different types of users.

when $B_2 = 5$, less than half users achieve an SIR of 0 dB with probability 80%; while when $B_2 = 100$, almost 80% users achieve the same SIR with probability 80%. In contrast, though the offloading does lower the SIR performance of those offloaded users, the degradation is quite small with the increase of B_2 owing to the avoidance of the inter-tier interference.

B. Rate Performance Trends

While the SINR performance is an important predictor of the user experience, it does not reveal the load on the BS, which is another critical factor. Therefore, in the following, we will investigate the user-perceived rate to illustrate the effect of joint offloading and resource allocation.

Fig. 5 shows how the shared fraction η_1 affects the standard per-tier rate coverage probability S_1 and the variance of the conditional per-tier rate coverage probability $S_2 - S_1^2$, where S_b is $S_{b|k}^{\mathrm{u}}$ or $S_{b|k}^{\mathrm{o}}$ according to the user type and the tier index. Apart from the similar observations to the SINR coverage, several new insights are revealed as follows: (1) since the user-perceived rate is closely related to the per-user available spectrum resource, increasing η_1 results in the performance enhancement for both MUs and the unoffloaded PUs but degradation for the offloaded PUs; (2) there is an obvious rate degradation for the offloaded PUs when B_2 increases even though the inter-tier interference is avoided, which implies the key impact of the resource

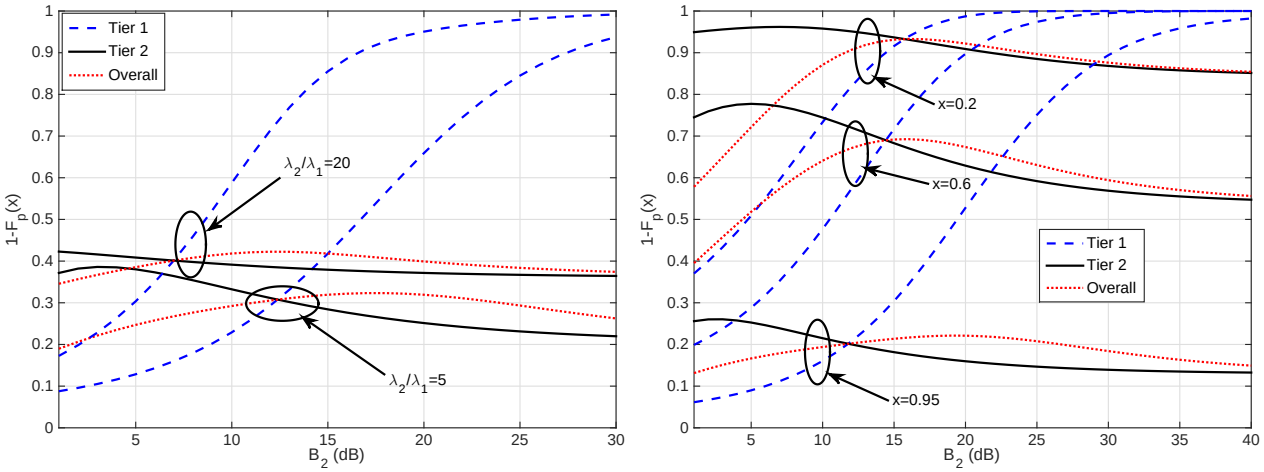

(a) The impact of density ratio for $x = 0.5$.

(b) Comparison of different target reliabilities x.

Fig. 6. The per-tier and overall rate meta distributions versus B_2 with $\eta_1 = \eta_2 = 0.5$.

allocation on the rate performance; (3) in spite of the degradation, the offloaded PUs still achieve a much higher performance than that without adopting the biased user association, which highlights the benefit of the load balancing. Fig. 5(b) plots the variance to show the degree of concentration for the conditional rate coverage probability. For a certain user type and B_2, there is always a maximum at some value of η_1, and the optimal η_1 is rather different for different types of users. In particular, the shape of the variance for MUs strongly depends on B_2.

Fig. 6 shows the per-tier and overall rate meta distributions as a function of B_2, where Fig. 6(a) and 6(b) study the impacts of the density ratio λ_2/λ_1 and the probability of achieving the target rate x, respectively. From both figures, we can see that the performance in tier 2 is much more stable than that in tier 1 with the increase of B_2 for different parameter settings. Thanks to the fine-grained analysis, we can see the significant performance improvement of MUs clearly. More importantly, we observe that the weighted averaged overall performance can neither reflect the remarkable enhancement in MU's performance nor the PU's stable performance. In most cases, it depends more on the load in each tier, or equivalently, the association probability. In addition, Fig. 6(a) also indicates that increasing the density ratio can further boost the rate performance of MUs while Fig. 6(b) tells us that irrespective of x, we can always make most MUs (e.g., more than 90%) achieve the target requirement through offloading.

Fig. 7 investigates how the mean load and the rate meta distribution in each tier change

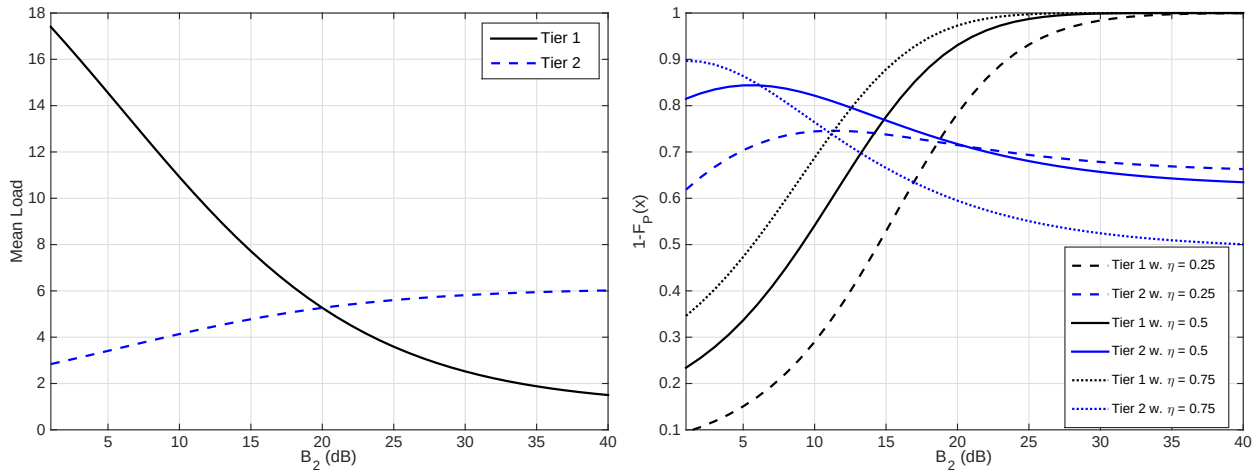

(a) Mean load in each tier vs. B_2.

(b) The rate meta distribution vs. B_2 for different η_1.

Fig. 7. The relationship between the mean load and the rate meta distribution in each tier with $x = 0.5$.

with the biasing factor B_2 and the relationship between them, where the mean load of the k-th tier is the mean number of the users served by the BSs in tier k and can be obtained by $\bar{N}_k = 1 + 1.28 A_k \lambda_{\mathrm{u}} / \lambda_k$ [4, Cor. 1]. It is seen that the biased user association can significantly reduce the load in tier 1 while the load in tier 2 grows slowly. Accordingly, in terms of the rate meta distribution, the performance fluctuation in tier 2 is much smaller than that in tier 1, which implies the critical effect of the load on the user-perceived rate performance. Furthermore, there also exists a close connection between the biasing factor and the fraction of the shared resource. When the available resource for the offloaded PUs is small (e.g., $\eta_1 = 0.75$), increasing B_2 means more users share this limited resource, thus reducing the robustness against the performance degradation. In this case, B_2 should not be chosen small or large: for the former, the performance of the unoffloaded user is much lower than that of the offloaded users, while the opposite is for the latter. As a result, setting B_2 near the intersection point between the two curves with $\eta_1 = 0.75$ makes users, either offloaded or unoffloaded, achieve almost identical performance. While for the other two cases of η_1, since the available resource is sufficient for the offloaded users relative to that for the unoffloaded ones, increasing B_2 does not have an obvious impact on the performance in tier 2 but still improves that in tier 1 significantly.

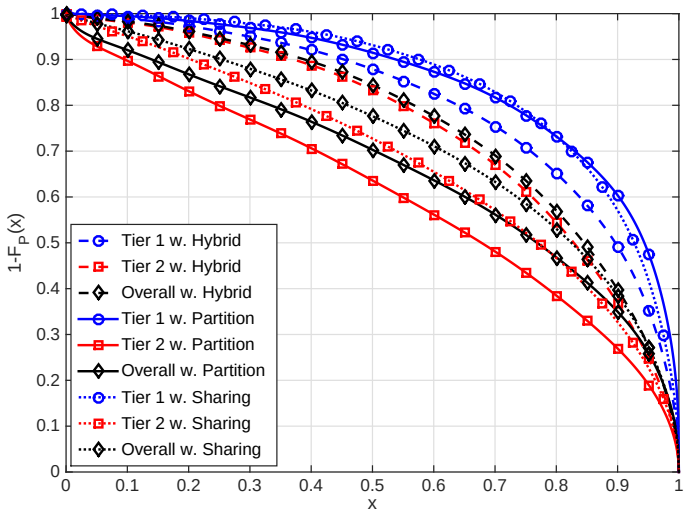

Fig. 8. The comparison of the rate meta distribution for different spectrum allocation schemes with $\lambda_2/\lambda_1 = 10$, $\lambda_u/\lambda_1 = 20$, and $\eta_1 = 0.75$.

C. Comparisons with Other Spectrum Allocation Schemes

Fig. 8 compares three different spectrum allocation schemes in terms of the per-tier and overall rate meta distributions, where the scheme adopted in this paper is referred to the hybrid one. In tier 1, the hybrid scheme achieves a lower rate performance of individual MUs than the other two schemes due to the cross-tier interference (compared with the spectrum partitioning) and the less spectrum resources (compared with the spectrum sharing). However, in all these three schemes, the fractions of MUs that achieve a target rate requirement with a certain probability are higher than those of PUs (in tier 2), which highlights the benefit of load balancing. Different from the MUs, the rate performance of individual PU using the hybrid scheme outperforms that of the other two schemes, which benefits from the usage of the entire spectrum band for the PUs and the avoidance of the inter-tier interference for the offloaded PUs. The overall performance is dominated by that of tier 2 since PUs account for the majority of the total users after offloading. Thus, the hybrid scheme gets the best overall rate performance.

Fig. 9 compares the conventional rate coverage probability with the rate meta distribution as a function of η_1 for the three spectrum allocation schemes. It is observed that with the same parameter setup, the two rate meta distributions under different target reliabilities, i.e., $x = 0.5$ in Fig. 9(b) and $x = 0.95$ in Fig. 9(c), yield rather different conclusions from each other as

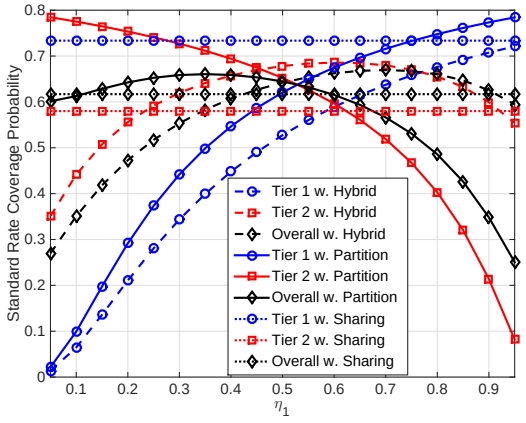

(a) The standard rate coverage probability vs. η_1.

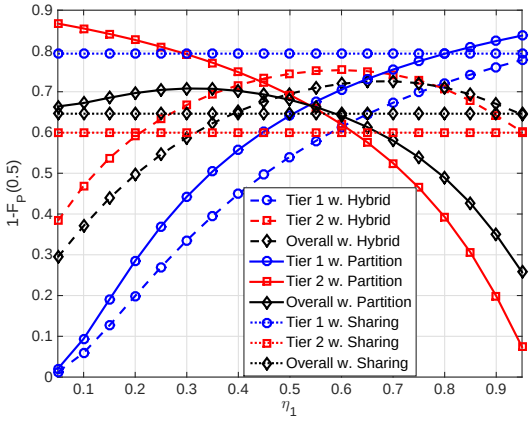

(b) The rate meta distribution vs. η_1 for $x = 0.5$.

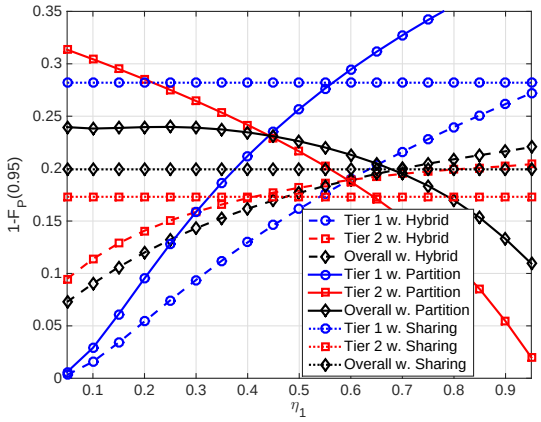

(c) The rate meta distribution vs. η_1 for $x = 0.95$.

Fig. 9. Comparison between the conventional rate coverage probability and the meta distribution for the hybrid, partition and sharing spectrum allocation schemes.

well as the standard rate coverage probability shown in Fig. 9(a). Specifically, in Fig. 9(b) for $x = 0.5$, the performance trends among the three strategies and the locations of the intersection points among the three curves for the hybrid and partition schemes are similar to those in Fig. 9(a). This is not surprising since Fig. 9(a) shows the mean and Fig. 9(b) the median of the meta distribution. However, the situation in Fig. 9(c) for $x = 0.95$ is quite different: (1) the values of η_1 corresponding to the intersection points are different; (2) the rate performance at the intersection point for the hybrid scheme is worse than the partition scheme, which is just opposite to the cases in the other two figures. These phenomena indicate that the conventional rate coverage

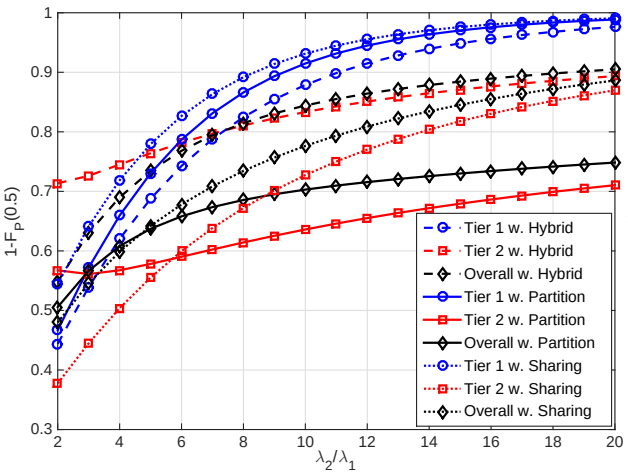

Fig. 10. The rate meta distribution vs. λ_2/λ_1 for $\lambda_{\rm u}/\lambda_1 = 20$, $x = 0.5$, and $\eta_1 = 0.75$.

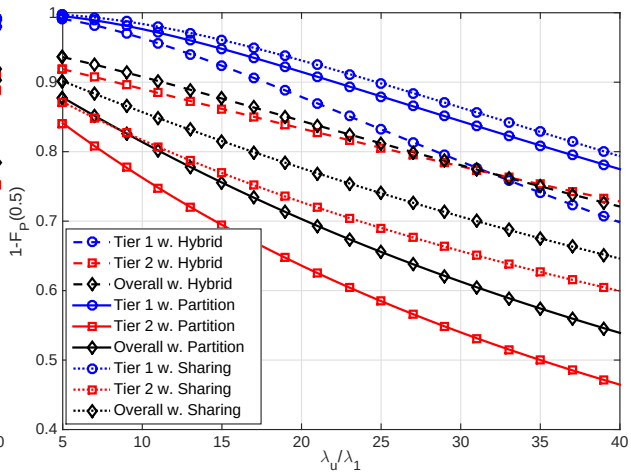

Fig. 11. The rate meta distribution vs. $\lambda_{\rm u}/\lambda_1$ for $\lambda_2/\lambda_1 = 10$, $x = 0.5$, and $\eta_1 = 0.75$.

probability cannot fully characterize the performance of individual users in the network. The impacts of spectrum allocation on the performance of the typical user and that of individual users can be rather different. In other words, for users that have different service experiences, the best choice of the spectrum allocation strategy and the optimal network parameters would be different, which should not be determined merely through the conventional rate coverage probability.

Fig. 10 investigates the impact of the density ratio on the rate meta distributions for the three spectrum allocation schemes. It is observed that increasing the density ratio improves the rate performance of individual users in each tier for all the three schemes. The increase of λ_2/λ_1 motivates more users to associate with tier 2 and reduces the load in each BS of both tiers. Accordingly, both MUs and PUs have more per-user resource and hence better performance. Furthermore, for the users in tier 2 and in the whole network, the hybrid one always achieves much better performance than the other two schemes due to the weaker interference (relative to the spectrum sharing) and the higher resource utilization (relative to the spectrum partitioning) which are two critical factors that affect the rate performance in HCNs. It is also seen that spectrum partitioning has a performance advantage at smaller density ratios while spectrum sharing has a performance advantage at larger density ratios.

Fig. 11 shows how the user density affects the rate meta distributions for the three spectrum

allocation schemes. As the user density increases, the per-user resource is decreased, resulting in the rate performance degradation and an approximately linear decline for the fraction of users that achieve the required rate with probability at least 50%. Compared with the other two schemes, the performance of the individual MUs in the hybrid scheme decreases faster while that of the individual PUs decreases more slowly. The reason is that MUs suffer from the cross-tier interference and the corresponding available resource is smaller than in the spectrum sharing scheme, while for PUs, the cross-tier interference is avoided for the offloaded PUs and the entire spectrum resource is available.

VI. Conclusions

While the SINR/rate performance evaluated at the typical user via spatial averaging is certainly important, it only provides limited information on the performance of individual users and hence cannot reflect the distribution of the performance of the users in a given realization of the network. To overcome this drawback, this paper provides an analytical framework for a fine-grained analysis of HCNs with joint offloading and resource partitioning based on the concept of the meta distribution. It is established that proper spectrum partitioning and offloading play an important role in radio resource management, and our work is the first to analyze the meta distribution of the SINR and user-perceived rate in a multi-tier HCN incorporating both of them. The availability of a functional form for the refined SINR and rate performance as functions of system parameters unlocks many avenues to gain deep design insights.

Using the developed analysis, the importance of combining load balancing with partial spectrum partitioning in terms of the meta distribution is clearly established. It is further shown that the per-tier performance is quite different from the overall performance; in other words, the overall performance through the spatial averaging cannot accurately reflect the performance of individual users in each tier. Moreover, the meta distribution yields important insights on proper choices for spectrum allocation strategies and biasing factors from the different service experiences of individual users in the network rather than the commonly evaluated average over all users. Therefore, it is necessary to use the meta distribution as a key refined metric to study these techniques in HCNs, and insights merely based on the spatial averages are inconclusive.

APPENDIX A
PROOF OF LEMMA 1

Proof: The probability that the typical user associates with the BS belonging to the k-th tier is

$$\begin{aligned} A_k &= \mathbb{P}(u_0 \in \mathcal{U}_k) \\ &= \mathbb{E}_{Z_k}\Big[\mathbb{P}\Big(\bigcap_{i\in[K]^!}\Big\{\mu_i B_i Z_i^{-\alpha_i} \le \mu_k B_k Z_k^{-\alpha_k}\Big\}\Big) \mid Z_k\Big] \\ &\overset{(a)}{=} \int_0^\infty \prod_{i\in[K]^!} \exp\Big(-\lambda_i\pi\Big(\frac{\mu_i B_i}{\mu_k B_k}\Big)^{2/\alpha_i} r^{2\alpha_k/\alpha_i}\Big) f_{Z_k}(r)\mathrm{d}r \\ &= \pi\lambda_k \int_0^\infty \exp\Big(-\sum_{i\in[K]} \pi\lambda_i(\hat{\mu}_{ik}\hat{B}_{ik})^{\delta_i} r^{\hat{\delta}_{ik}}\Big)\mathrm{d}r, \end{aligned} \tag{39}$$

where step (a) follows from the empty space function of the PPP [19] and $f_{Z_k}(r) = 2\pi\lambda_k r e^{-\lambda_k\pi r^2}$ is the distribution of the nearest distance Z_k [22]. Then, the probability that the typical user is unoffloaded, i.e., $u_0 \in \mathcal{U}_k^{\mathrm{u}}$, can be further given as

$$\begin{aligned} A_k^{\mathrm{u}} &= \mathbb{P}(u_0 \in \mathcal{U}_k) \\ &= \mathbb{E}_{Z_k}\Big[\mathbb{P}\Big(\bigcap_{i<k}\Big\{\mu_i Z_i^{-\alpha_i} \le \mu_k Z_k^{-\alpha_k}\Big\}\bigcap_{i>k}\Big\{\mu_i B_i Z_i^{-\alpha_i} \le \mu_k B_k Z_k^{-\alpha_k}\Big\}\Big) \mid Z_k\Big] \\ &= \pi\lambda_k \int_0^\infty \exp\Big(-\sum_{i\le k} \pi\lambda_i \hat{\mu}_{ik}^{\delta_i} r^{\hat{\delta}_{ik}} - \sum_{i>k} \pi\lambda_i(\hat{\mu}_{ik}\hat{B}_{ik})^{\delta_i} r^{\hat{\delta}_{ik}}\Big)\mathrm{d}r. \end{aligned} \tag{40}$$

According to the total probability law, we have $A_k^{\mathrm{o}} = A_k - A_k^{\mathrm{u}}$. ■

APPENDIX B
PROOF OF LEMMA 2

Proof: We first derive the CCDF of the distance between the typical user and its serving BS. Given $u_0 \in \mathcal{U}_k$, we have

$$\begin{aligned} \mathbb{P}(Z_k > r \mid u_0 \in \mathcal{U}_k) &= \frac{\mathbb{P}(Z_k > r, u_0 \in \mathcal{U}_k)}{A_k} \\ &= \frac{1}{A_k}\int_r^\infty \mathbb{P}\Big(\bigcap_{i\in[K]^!}\Big\{\mu_i B_i Z_i^{-\alpha_i} \le \mu_k B_k Z_k^{-\alpha_k}\Big\}\Big) f_{Z_k}(t)\mathrm{d}t \\ &= \frac{2\pi\lambda_k}{A_k}\int_r^\infty \exp\Big(-\sum_{i\in[K]} \pi\lambda_i(\hat{\mu}_{ik}\hat{B}_{ik})^{\delta_i} t^{2\hat{\delta}_{ik}}\Big)\mathrm{d}t. \end{aligned} \tag{41}$$

Furthermore, given $u_0 \in \mathcal{U}_k^{\mathrm{u}}$, we have

$$\begin{aligned}\mathbb{P}(Z_k > r \mid u_0 \in \mathcal{U}_k^{\mathrm{u}}) &= \frac{\mathbb{P}(Z_k > r, u_0 \in \mathcal{U}_k^{\mathrm{u}})}{A_k^{\mathrm{u}}} \\ &= \frac{1}{A_k^{\mathrm{u}}} \int_r^{\infty} \mathbb{P}\Big(\bigcap_{i<k} \Big\{ \mu_i Z_i^{-\alpha_i} \le \mu_k t^{-\alpha_k} \Big\} \bigcap_{i>k} \Big\{ \mu_i B_i Z_i^{-\alpha_i} \le \mu_k B_k t^{-\alpha_k} \Big\} \Big) f_{Z_k}(t) \mathrm{d}t \\ &= \frac{2\pi\lambda_k}{A_k^{\mathrm{u}}} \int_r^{\infty} \exp\Big(- \sum_{i\le k} \pi\lambda_i \hat{\mu}_{ik}^{\delta_i} t^{2\hat{\delta}_{ik}} - \sum_{i>k} \pi\lambda_i (\hat{\mu}_{ik}\hat{B}_{ik})^{\delta_i} t^{2\hat{\delta}_{ik}} \Big) \mathrm{d}t. \end{aligned} \tag{42}$$

Given $u_0 \in \mathcal{U}_k^{\mathrm{o}}$, we have

$$\begin{aligned}\mathbb{P}(Z_k > r \mid u_0 \in \mathcal{U}_k^{\mathrm{o}}) &= \frac{\mathbb{P}(Z_k > r, u_0 \in \mathcal{U}_k) - \mathbb{P}(Z_k > r, u_0 \in \mathcal{U}_k^{\mathrm{u}})}{A_k^{\mathrm{o}}} \\ &= \frac{2\pi\lambda_k}{A_k^{\mathrm{o}}} \int_r^{\infty} \exp\Big(- \sum_{i\in[K]} \pi\lambda_i (\hat{\mu}_{ik}\hat{B}_{ik})^{\delta_i} t^{2\hat{\delta}_{ik}} \Big) \\ &\quad - \exp\Big(- \sum_{i\le k} \pi\lambda_i \hat{\mu}_{ik}^{\delta_i} t^{2\hat{\delta}_{ik}} - \sum_{i>k} \pi\lambda_i (\hat{\mu}_{ik}\hat{B}_{ik})^{\delta_i} t^{2\hat{\delta}_{ik}} \Big) \mathrm{d}t. \end{aligned} \tag{43}$$

The corresponding PDFs $f_{Z_k|u_0\in\mathcal{U}_k}(r)$,$f_{Z_k|u_0\in\mathcal{U}_k^{\mathrm{u}}}(r)$, and $f_{Z_k|u_0\in\mathcal{U}_k^{\mathrm{o}}}(r)$ are the derivatives of Eq. (41)-(43) with respect to r, respectively. ■

APPENDIX C
PROOF OF THEOREM 1

Proof: Given that the typical user is served by a BS in the k-th tier with $u_0 \in \mathcal{U}_k^{\mathrm{u}}$, the conditional success probability is

$$\begin{aligned} &\mathbb{P}(\mathrm{SINR}_k > \theta \mid \Phi, u_0 \in \mathcal{U}_k^{\mathrm{u}}) \\ &= \mathbb{P}\Big(\frac{\mu_k \ell_k(Z_k) h_{x_0}}{\sum\limits_{x\in\Phi_k^!} \mu_k \ell_k(x) h_x + \sum\limits_{i\in[K]^!} \sum\limits_{x\in\Phi_i} \mu_i \ell_i(x) h_x + \sigma^2} > \theta \mid \Phi, u_0 \in \mathcal{U}_k^{\mathrm{u}} \Big) \\ &= \mathbb{E}\Big[\exp\Big(- \frac{\theta Z_k^{\alpha_k}}{\mu_k} \Big(\sum_{x\in\Phi_k^!} \mu_k \ell_k(x) h_x + \sum_{i\in[K]^!} \sum_{x\in\Phi_i} \mu_i \ell_i(x) h_x + \sigma^2 \Big) \Big) \mid \Phi, u_0 \in \mathcal{U}_k^{\mathrm{u}} \Big] \\ &= e^{-\frac{\sigma^2}{\mu_k}\theta Z_k^{\alpha_k}} \prod_{x\in\Phi_k^!} \frac{1}{1+\theta Z_k^{\alpha_k}|x|^{-\alpha_k}} \prod_{i\in[K]^!} \prod_{x\in\Phi_i} \frac{1}{1+\theta\hat{\mu}_{ik} Z_k^{\alpha_k}|x|^{-\alpha_i}}. \end{aligned} \tag{44}$$

Then, the b-th moment follows as

$$M_{b|k}^{\mathrm{u}}(\theta) \;=\; \mathbb{E}\Big[\mathbb{P}(\mathrm{SINR}_k > \theta \mid \Phi, u_0 \in \mathcal{U}_k^{\mathrm{u}})^b \Big]$$

$$
\begin{aligned}
&= \mathbb{E}\Big[e^{-\frac{b\sigma^2}{\mu_k}\theta Z_k^{\alpha_k}}\prod_{x\in\Phi_k^!}\frac{1}{(1+\theta Z_k^{\alpha_k}|x|^{-\alpha_k})^b}\prod_{i\in[K]^!}\prod_{x\in\Phi_i}\frac{1}{(1+\theta\hat{\mu}_{ik}Z_k^{\alpha_k}|x|^{-\alpha_i})^b}\Big]\\
&\overset{(a)}{=} \int_0^\infty f_{Z_k|u_0\in\mathcal{U}_k^{\mathrm{u}}}(r)e^{-\frac{\sigma^2 b\theta}{\mu_k}r^{\alpha_k}}\exp\Big(-2\pi\sum_{i\le k}\lambda_i\int_{\hat{\mu}_{ik}^{\frac{1}{\alpha_i}}r^{\frac{\alpha_k}{\alpha_i}}}^\infty\big(1-(1+\theta\hat{\mu}_{ik}r^{\alpha_k}t^{-\alpha_i})^{-b}\big)t\mathrm{d}t\\
&\quad -2\pi\sum_{i>k}\lambda_i\int_{(\hat{B}_{ik}\hat{\mu}_{ik})^{\frac{1}{\alpha_i}}r^{\frac{\alpha_k}{\alpha_i}}}^\infty\big(1-(1+\theta\hat{\mu}_{ik}r^{\alpha_k}t^{-\alpha_i})^{-b}\big)t\mathrm{d}t\Big)\mathrm{d}r\\
&= \int_0^\infty f_{Z_k|u_0\in\mathcal{U}_k^{\mathrm{u}}}(r)e^{-\frac{\sigma^2 b\theta}{\mu_k}r^{\alpha_k}}\exp\Big(-2\pi\sum_{i\le k}\lambda_i\hat{\mu}_{ik}^{\delta_i}r^{2\hat{\delta}_{ik}}\int_0^1\big(1-(1+\theta t^{\alpha_i})^{-b}\big)t^{-3}\mathrm{d}t\\
&\quad -2\pi\sum_{i>k}\lambda_i(\hat{B}_{ik}\hat{\mu}_{ik})^{\delta_i}r^{2\hat{\delta}_{ik}}\int_0^1\big(1-(1+\theta\hat{B}_{ik}^{-1}t^{\alpha_i})^{-b}\big)t^{-3}\mathrm{d}t\Big)\mathrm{d}r\\
&= \frac{2\pi\lambda_k}{A_k^{\mathrm{u}}}\int_0^\infty e^{-\frac{\sigma^2 b\theta}{\mu_k}r^{\alpha_k}}\exp\Big(-\pi\sum_{i\le k}\lambda_i\hat{\mu}_{ik}^{\delta_i}r^{2\hat{\delta}_{ik}}\Big[1+2\int_0^1\big(1-(1+\theta t^{\alpha_i})^{-b}\big)t^{-3}\mathrm{d}t\Big]\\
&\quad -\pi\sum_{i>k}\lambda_i(\hat{B}_{ik}\hat{\mu}_{ik})^{\delta_i}r^{2\hat{\delta}_{ik}}\Big[1+2\int_0^1\big(1-(1+\theta\hat{B}_{ik}^{-1}t^{\alpha_i})^{-b}\big)t^{-3}\mathrm{d}t\Big]\Big)\mathrm{d}r\\
&= \frac{\pi\lambda_k}{A_k^{\mathrm{u}}}\int_0^\infty e^{-\frac{\sigma^2 b\theta}{\mu_k}r^{\frac{\alpha_k}{2}}}\exp\Big(-\pi\sum_{i\le k}\lambda_i\hat{\mu}_{ik}^{\delta_i}r^{\hat{\delta}_{ik}}F_b(\alpha_i,b)\\
&\quad -\pi\sum_{i>k}\lambda_i(\hat{B}_{ik}\hat{\mu}_{ik})^{\delta_i}r^{\hat{\delta}_{ik}}F_b(\alpha_i,\hat{B}_{ik}^{-1}\theta)\Big)\mathrm{d}r, \qquad (45)
\end{aligned}
$$

where step (a) follows from the probability generating functional (PGFL) of the PPP [19], and the integration limits are obtained since the closest interferer in the i-th tier satisfies (2).

Given that the typical user is served by a BS in the k-th tier with $u_0 \in \mathcal{U}_k^{\mathrm{o}}$, the conditional success probability is

$$
\begin{aligned}
\mathbb{P}(\mathrm{SINR}_k > \theta \mid \Phi, u_0 \in \mathcal{U}_k^{\mathrm{o}}) &= \mathbb{P}\Big(\frac{\mu_k\ell_k(Z_k)h_{x_0}}{\sum_{x\in\Phi_k^!}\mu_k\ell_k(x)h_x+\sigma^2} > \theta \mid \Phi, u_0\in\mathcal{U}_k^{\mathrm{o}}\Big)\\
&= e^{-\frac{\sigma^2}{\mu_k}\theta Z_k^{\alpha_k}}\prod_{x\in\Phi_k^!}\frac{1}{1+\theta Z_k^{\alpha_k}|x|^{-\alpha_k}}. \qquad (46)
\end{aligned}
$$

Hence, the b-th moment follows as

$$
\begin{aligned}
M_{b|k}^{\mathrm{o}}(\theta) &= \mathbb{E}\Big[\mathbb{P}(\mathrm{SINR}_k > \theta \mid \Phi, u_0\in\mathcal{U}_k^{\mathrm{o}})^b\Big]\\
&= \int_0^\infty f_{Z_k|u_0\in\mathcal{U}_k^{\mathrm{o}}}(r)e^{-\frac{\sigma^2 b\theta}{\mu_k}r^{\alpha_k}}\exp\Big(-2\pi\lambda_k\int_r^\infty\big(1-(1+\theta r^{\alpha_k}t^{-\alpha_k})^{-b}\big)t\mathrm{d}t\Big)\mathrm{d}r
\end{aligned}
$$

$$= \int_0^\infty f_{Z_k|u_0\in\mathcal{U}_k^{\mathrm{o}}}(r) e^{-\frac{\sigma^2 b\theta}{\mu_k} r^{\alpha_k}} \exp\Big(-2\pi\lambda_k r^2 \int_0^1 \big(1-(1+\theta t^{\alpha_k})^{-b}\big) t^{-3}\mathrm{d}t\Big)\mathrm{d}r$$

$$= \frac{\pi\lambda_k}{A_k^{\mathrm{o}}} \int_0^\infty e^{-\frac{b\sigma^2\theta}{\mu_k} r^{\frac{\alpha_k}{2}}} \exp\Big(-\sum_{i>k}\pi\lambda_i(\hat{\mu}_{ik}\hat{B}_{ik})^{\delta_i} r^{\hat{\delta}_{ik}} - \pi\lambda_k F_b(\alpha_k,\theta) r\Big)$$

$$\times\Bigg[\exp\Big(-\sum_{i<k}\pi\lambda_i(\hat{\mu}_{ik}\hat{B}_{ik})^{\delta_i} r^{\hat{\delta}_{ik}}\Big) - \exp\Big(-\sum_{i<k}\pi\lambda_i\hat{\mu}_{ik}^{\delta_i} r^{\hat{\delta}_{ik}}\Big)\Bigg]\mathrm{d}r. \tag{47}$$

Finally, we have the per-tier moment

$$\begin{aligned} M_{b|k}(\tau) &= \mathbb{E}\Bigg[\mathbb{P}\Big(\mathrm{SINR}_k > \theta \mid u_0 \in \mathcal{U}_k, \Phi\Big)^b\Bigg] \\ &\overset{(b)}{=} \frac{\mathbb{P}(u_0\in\mathcal{U}_k^{\mathrm{u}})}{\mathbb{P}(u_0\in\mathcal{U}_k)} \mathbb{E}\Bigg[\mathbb{P}\Big(\mathrm{SINR}_k > \theta \mid u_0 \in \mathcal{U}_k^{\mathrm{u}}, \Phi\Big)^b\Bigg] \\ &\quad + \frac{\mathbb{P}(u_0\in\mathcal{U}_k^{\mathrm{o}})}{\mathbb{P}(u_0\in\mathcal{U}_k)} \mathbb{E}\Bigg[\mathbb{P}\Big(\mathrm{SINR}_k > \theta \mid u_0 \in \mathcal{U}_k^{\mathrm{o}}, \Phi\Big)^b\Bigg] \\ &= \frac{1}{A_k}\big(A_k^{\mathrm{u}} M_{b|k}^{\mathrm{u}}(\theta) + A_k^{\mathrm{o}} M_{b|k}^{\mathrm{o}}(\theta)\big), \end{aligned} \tag{48}$$

where step (b) follows the total probability law. ■

REFERENCES

[1] N. Deng and M. Haenggi, "The meta distribution of the SINR and rate in heterogeneous cellular networks," in *Proc. 29th IEEE PIMRC*, Bologna, Italy, Sept. 2018, accepted.

[2] J. G. Andrews, "Seven ways that HetNets are a cellular paradigm shift," *IEEE Commun. Mag.*, vol. 51, no. 3, pp. 136–144, Mar. 2013.

[3] 3GPP, "Evolved Universal Terrestrial Radio Access (E-UTRA); User Equipment (UE) conformance specification; Radio transmission and reception; Part 1: Conformance Testing," 3rd Generation Partnership Project (3GPP), Technical Specification (TS) 36.521-1, Mar. 2018, version 15.1.1.

[4] S. Singh, H. S. Dhillon, and J. G. Andrews, "Offloading in heterogeneous networks: Modeling, analysis, and design insights," *IEEE Trans. Wireless Commun.*, vol. 12, no. 5, pp. 2484–2497, May 2013.

[5] S. Singh and J. G. Andrews, "Joint resource partitioning and offloading in heterogeneous cellular networks," *IEEE Trans. Wireless Commun.*, vol. 13, no. 2, pp. 888–901, Feb. 2014.

[6] W. Bao and B. Liang, "Rate maximization through structured spectrum allocation and user association in heterogeneous cellular networks," *IEEE Trans. Commun.*, vol. 63, no. 11, pp. 4510–4524, Nov. 2015.

[7] M. Haenggi, "The mean interference-to-signal ratio and its key role in cellular and amorphous networks," *IEEE Wireless Commun. Lett.*, vol. 3, no. 6, pp. 597–600, Dec. 2014.

[8] H. S. Jo, Y. J. Sang, P. Xia, and J. G. Andrews, "Heterogeneous cellular networks with flexible cell association: A comprehensive downlink SINR analysis," *IEEE Trans. Wireless Commun.*, vol. 11, no. 10, pp. 3484–3495, Oct. 2012.

[9] S. Mukherjee, "Distribution of downlink SINR in heterogeneous cellular networks," *IEEE J. Sel. Areas Commun.*, vol. 30, no. 3, pp. 575–585, Apr. 2012.

[10] Kyocera, "Potential performance of range expansion in macro-pico deployment," 3rd Generation Partnership Project (3GPP), TSG RAN WG1 Meeting-62 R1-104355, Aug. 2010.

[11] S. Sadr and R. S. Adve, "Tier association probability and spectrum partitioning for maximum rate coverage in multi-tier heterogeneous networks," *IEEE Commun. Lett.*, vol. 18, no. 10, pp. 1791–1794, Oct. 2014.

[12] Y. Lin, W. Bao, W. Yu, and B. Liang, "Optimizing user association and spectrum allocation in hetnets: A utility perspective," *IEEE J. Sel. Areas Commun.*, vol. 33, no. 6, pp. 1025–1039, Jun. 2015.

[13] M. Haenggi, "The meta distribution of the SIR in Poisson bipolar and cellular networks," *IEEE Trans. Wireless Commun.*, vol. 15, no. 4, pp. 2577–2589, Apr. 2016.

[14] M. Salehi, A. Mohammadi, and M. Haenggi, "Analysis of D2D underlaid cellular networks: SIR meta distribution and mean local delay," *IEEE Trans. Commun.*, vol. 65, no. 7, pp. 2904–2916, Jul. 2017.

[15] N. Deng and M. Haenggi, "A fine-grained analysis of millimeter-wave device-to-device networks," *IEEE Trans. Commun.*, vol. 65, no. 11, pp. 4940–4954, Nov. 2017.

[16] Y. Wang, M. Haenggi, and Z. Tan, "The meta distribution of the SIR for cellular networks with power control," *IEEE Transactions on Communications*, vol. 66, no. 4, pp. 1745–1757, Apr. 2018.

[17] Q. Cui, X. Yu, Y. Wang, and M. Haenggi, "The SIR meta distribution in Poisson cellular networks with base station cooperation," *IEEE Trans. Commun.*, vol. 66, no. 3, pp. 1234–1249, Mar. 2018.

[18] Y. Wang, M. Haenggi, and Z. Tan, "SIR meta distribution of K-tier downlink heterogeneous cellular networks with cell range expansion," *arXiv preprint arXiv:1803.00182*, 2018.

[19] M. Haenggi, *Stochastic geometry for wireless networks*. Cambridge University Press, 2012.

[20] ——, "Efficient calculation of meta distributions and the performance of user percentiles," *IEEE Wireless Commun. Lett.*, 2018, available on IEEE Xplore Early Access.

[21] S. Guruacharya and E. Hossain, "Approximation of meta distribution and its moments for Poisson cellular networks," *IEEE Wireless Commun. Lett.*, 2018, available on IEEE Xplore Early Access.

[22] M. Haenggi, "On distances in uniformly random networks," *IEEE Trans. Inf. Theory*, vol. 51, no. 10, pp. 3584–3586, Oct. 2005.